Chemical Engineering Communications
Publication details, including instructions for authors and subscription information:
http://www.informaworld.com/smpp/title~content=t713454788

CAPILLARY NETWORK MODELS FOR TRANSPORT IN PACKED BEDS: CONSIDERATIONS OF PORE ASPECT RATIO

Suresh K. Bhatia[a]
[a] Department of Chemical Engineering, Indian Institute of Technology, Powai, Bombay, India

To cite this Article Bhatia, Suresh K.(1996) 'CAPILLARY NETWORK MODELS FOR TRANSPORT IN PACKED BEDS: CONSIDERATIONS OF PORE ASPECT RATIO', Chemical Engineering Communications, 154: 1, 183 — 202
To link to this Article: DOI: 10.1080/00986449608936651
URL: http://dx.doi.org/10.1080/00986449608936651

Chem. Eng. Comm., 1996, Vol. 154, pp. 183–202
Reprints available directly from the publisher
Photocopying permitted by license only

CAPILLARY NETWORK MODELS FOR TRANSPORT IN PACKED BEDS: CONSIDERATIONS OF PORE ASPECT RATIO

SURESH K. BHATIA

Department of Chemical Engineering, Indian Institute of Technology, Powai, Bombay 400 076, India

(Received August 1, 1995; in final form March 27, 1996)

The conventional analysis for the estimation of the tortuosity factor for transport in porous media is modified here to account for the effect of pore aspect ratio. Structural models of the porous medium are also constructed for calculating the aspect ratio as a function of porosity. Comparison of the model predictions with the extensive data of Currie (1960) for the effective diffusivity of hydrogen in packed beds shows good agreement with a network model of randomly oriented intersecting pores for porosities upto about 50 percent, which is the region of practical interest. The predictions based on this network model are also found to be in better agreement with the data of Currie than earlier expressions developed for unconsolidated and grainy media.

KEYWORDS Pore network Diffusion Packed bed Aspect ratio Porous media

INTRODUCTION

The mathematical modelling of transport processes in porous materials is of concern in a large variety of applications, and has attracted considerable interest in the chemical engineering literature. The most common approach in the modelling utilizes an effective transport coefficient in conjuction with the flux law

$$J = K_e \nabla q \tag{1}$$

where ∇q is a driving force. Various theories have been developed for the estimation of the effective transport coefficient K_e in terms of molecular and bulk properties of the fluid and structural properties of the porous medium (Jackson, 1977; Mason *et al.*, 1983; Bhatia, 1985; 1986; Burganos and Sotirchos, 1987; Sahimi *et al.*, 1990; Deepak and Bhatia, 1994), and the majority of these rely on the idealized representation of the pore space in terms of a network of cylindrical capillaries. This forms one of the simplest models of the porous medium and in general leads to a relation for the effective transport coefficient of the form

$$K_e = \frac{\varepsilon \bar{K}}{\gamma} \tag{2}$$

New Address: Department of Chemical Engineering, The University of Queensland, Brisbane, QLD 4072, Australia.

where γ is a tortuosity factor and $\bar{K}$ a suitably averaged mean pore conductivity. Under conditions when K is independent of pore size, such as in liquid phase diffusion or the molecular regime for gas phase diffusion, the sole unknown in the tortuosity factor which must now depend only on the porous medium structure. The most widely accepted value for the tortuosity is $\gamma = 3$ based on a random pore orientation (Johnson and Stewart, 1965), although corrections to this allowing for correlation among successive pores traversed have also appeared (Bhatia, 1985, 1986).

The above approach for estimating transport coefficients, while commonly used for consolidated media such as porous catalyst particles and adsorbents, has hitherto had limited success with unconsolidated media such as packed beds. For such cases it is more common to use earlier well-known results which do not consider a pore network idealization, but instead emphasize the grainy nature of the medium (Rayleigh, 1892; Maxwell, 1892; Bruggemann, 1935; Meredith and Tobias, 1961; Prager, 1963; Weissberg, 1963). However, as will be seen, even these are generally unsatisfactory, and the extension of the network models to unconsolidated solids is therefore a potentially attractive problem. The most important cause of deviations in the latter case is the assumption of purely axial transport in the pores inherent to the studies referred to above. In pores of finite radius and aspect ratio (defined here as the pore radius to length ratio) greater than zero this need not be the case, so that a more detailed analysis is necessary for estimating the tortuosity. This is particularly important for grainy unconsolidated media where the aspect ratio can be of the order of unity. The need for such an analysis is also evident from the requirement that for molecular transport $\gamma \to 1$ as $\varepsilon \to 1$, which is not satisfied by the conventional theory based on axial transport in the pores. While simulative approaches consistent with this requirement have been published (Akanni *et al.*, 1987; Tomadakis and Sotirchos, 1993) the development of an analytical result which is computationally much less demanding is also desirable.

A rigorous treatment of the problem would incorporate radial and axial transport within the pores, considering these as a small scale phenomenon, embedded within the larger scale random walk between pore intersections (Bhatia, 1985, 1986). This kind of complexity will lead to a computationally demanding theory, as is the case even for the result with the radial gradients neglected (Bhatia, 1986). However, a more tractable approach is suggested by the work of Pismen (1974) who assumed that in pores of finite radius the resulting transport direction is that closest to the macroscopic one. In his analysis, however, Pismen made the ad-hoc assumption that $r/\ell = \varepsilon^{1/2}$ for any pore, which at best is only an order of magnitude estimate. A more justifiable approach would be to construct structural models of the porous medium and develop the precise aspect ratio-porosity relationships based on these, which may then be used in the transport modelling. This is the approach adopted in the present article in which we investigate the variation of effective transport coefficient with porosity for three different structural models. These include a network of pores in a cubic lattice, another with randomly oriented pore segments, and one with randomly overlapping capillaries, each having a uniform pore size. While the development is done for the case of molecular diffusion the results are valid for any transport process taking place in the pores, in which the local transport coefficient is

independent of pore size. As will be subsequently seen additional complications arise when the local transport coefficient varies with pore size, as for Knudsen diffusion, and this case is therefore not considered here. The results obtained here are compared with a large amount of data for diffusion in packed beds (Currie, 1960), and yield better agreement than those of the earlier theories for transport in unconsolidated porous media.

THEORY

Transport Model

Small aspect ratio

We develop the transport model under the assumption of uniformly sized pores. In the conventional transport models the tortuosity factor γ in Eq. (2) is estimated from (Johnson and Stewart, 1965)

$$\gamma^{-1} = \langle \cos^2(\theta) \rangle \tag{3}$$

in which $\langle \cdot \rangle$ represents an orientational averaging of the angle θ, which represents the angle between the net diffusion direction in a pore and the macroscopic flux vector. If it is assumed that diffusion in a pore proceeds axially then the probability distribution for θ is the same as that for the pore axis. For a random pore orientation

$$p(\theta) = \frac{1}{2}\sin(\theta), \quad 0 \leqslant \theta \leqslant \pi \tag{4}$$

and it readily follows from Eqs. (3) and (4) that $\gamma = 3$. As a modification of the above analysis it has been recognized (Bhatia, 1985; 1986) that all pores traversed by diffusing molecules are not necessarily random, as the meandering motion can result in retracing of the path. Consequently successive pores traversed are correlated. Such an effect is well known in solid-state diffusion wherein a molecule diffusing by a site to site hopping mechanism has a finite probability of returning to the site just vacated (Le Claire, 1976). This effect is most conveniently captured by the correlation factor (Le Claire, 1976)

$$F = \frac{1 + \langle \cos(\theta_c) \rangle}{1 - \langle \cos(\theta_c) \rangle} \tag{5}$$

in which θ_c is the angle between successive steps in the random walk between pore intersections in a network. In terms of this correlation factor the tortuosity expression in Eq. (3) is now modified to (Bhatia, 1985)

$$\gamma^{-1} = F \langle \cos^2(\theta) \rangle \tag{6}$$

For purely axial transport in a pore $\theta_c = \pi$ and $\cos(\theta_c) = -1$ when a molecule re-traverses the pore after having just diffused through it. In a cubic network of uniformly sized pores there is always a pore also in the forward direction for which $\cos(\theta_c) = 1$, and it is easily seen that $\langle \cos(\theta_c) \rangle = 0$. This is also the case for randomly

overlapping capillaries. However, for a network of randomly oriented segments $\cos(\theta_c) = 0$ for all but the pore just traversed, for which $\cos(\theta_c) = -1$. When all pores are of uniform size the probability is $1/N$ that the molecule retraces its path, so that $\langle \cos\theta_c \rangle = -1/N$, and

$$F = \frac{N-1}{N+1} \tag{7}$$

Finite aspect ratio

To incorporate the effect of finite pore size in the above analysis we assume following Pismen (1974) that the net diffusion direction in a pore is that closest to the macroscopic flux vector. Thus, following the situation depicted in Figure 1, we have

$$\theta = 0 \quad \text{for} \quad \theta_2 \leqslant \theta_1 \tag{8}$$

$$\theta = \theta_2 - \theta_1 \quad \text{for} \quad \theta_1 \leqslant \theta_2 < \pi/2 \tag{9}$$

$$\theta = \theta_1 + \theta_2 \quad \text{for} \quad \frac{\pi}{2} < \theta_2 \leqslant \pi - \theta_1 \tag{10}$$

$$\theta = \pi \quad \text{for} \quad \pi - \theta_1 \leqslant \theta_2 \leqslant \pi \tag{11}$$

in which θ_1 is defined such that $\tan(\theta_1) = 2r/\ell$, and θ_2 is the angle between the macroscopic diffusion direction and the pore axis. The average value of $\cos^2(\theta)$ over

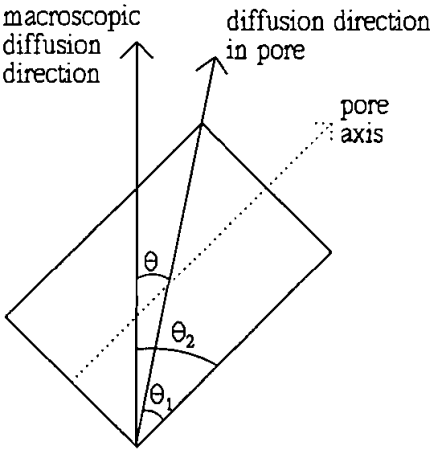

FIGURE 1 Diffusion direction in a pore.

all pore orientations, with the probability distribution for θ_2 following Eq. (4), is easily seen to be given by

$$\langle \cos^2(\theta) \rangle = \int_0^{\pi} \cos^2(\theta) \frac{\sin(\theta_2)}{2} d\theta_2$$

$$= 1 + \frac{4X}{3(1+4X^2)} - \frac{2}{3(1+4X^2)^{1/2}} \tag{12}$$

which has the property that $\langle \cos^2(\theta) \rangle \to 1$ as $X(=r/\ell) \to \infty$. This is also the limit to be expected as $\varepsilon \to 1$, as in this case the effective pore length must reduce to zero as a result of intersection and overlap. Figure 2 depicts the variation of tortuosity with pore aspect ratio X, following Eqs. (6) and (12), with the correlation factor F taken to be unity. Starting from $X = 0$, at which point $\gamma = 3$, there is a rapid decrease in the tortuosity with the value dropping to about 1.03 at $X = 1$. This underscores the importance of accounting for a non-zero pore aspect ratio in the transport modelling.

As mentioned above the correlation factor F in Eqs. (5) and (6) is unity for symmetric networks such as cubic or randomly overlapping capillary systems. For other networks, such as those comprising of randomly oriented pore segments, it is necessary to estimate this factor by means of Eq. (5). To this end we first estimate the average value of $\cos(\theta_c)$ for a pore of non-zero radius. For this purpose we assume that a molecule can enter the pore at any random location on the cross-section with a uniform probability, and leave the pore from any point randomly located on the opposite cross-section. Similarly on return the molecule can re-enter and exit from any random location on the corresponding planes. Referring to

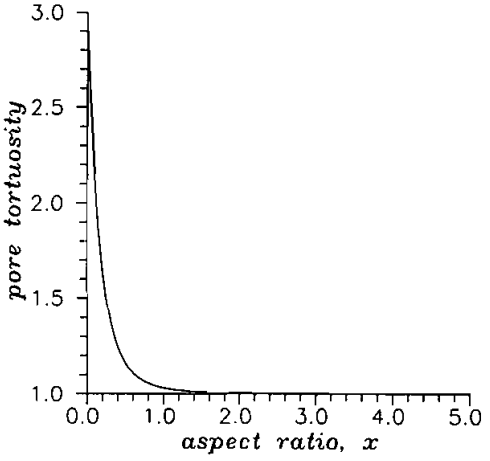

FIGURE 2 Variation of pore tortuosity with aspect ratio X, predicted by Eq. (12).

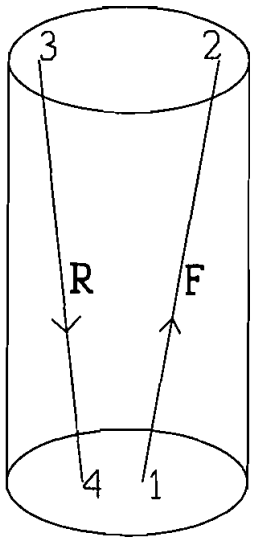

FIGURE 3 Forward and reverse displacement vectors in a pore.

Figure 3 we denote **F** and **R** as the forward and reverse displacement vectors, given in cylindrical coordinates as

$$\mathbf{F} = [r_2\cos(\alpha_2) - r_1\cos(\alpha_1)]\mathbf{i} + [r_2\sin(\alpha_2) - r_1\sin(\alpha_1)]\mathbf{j} + \ell\mathbf{k} \tag{13}$$

$$\mathbf{R} = [r_4\cos(\alpha_4) - r_3\cos(\alpha_3)]\mathbf{i} + [r_4\sin(\alpha_4) - r_3\sin(\alpha_3)]\mathbf{j} - \ell\mathbf{k} \tag{14}$$

in which (r_i, α_i, z_i) refer to the coordinates of the ith point. The value of $\cos(\theta_c)$ is now readily obtained from

$$\cos(\theta_c) = \frac{\mathbf{F}.\mathbf{R}}{\sqrt{\mathbf{F}.\mathbf{F}}\sqrt{\mathbf{R}.\mathbf{R}}} \tag{15}$$

whose average over the locations of points 1, 2, 3 and 4 is given by

$$\overline{\cos(\theta_c)} = \int_0^{2\pi}\int_0^{2\pi}\int_0^{2\pi}\int_0^{2\pi}\int_0^{r}\int_0^{r}\int_0^{r}\int_0^{r}\cos(\theta_c)\frac{[\prod_{i=1}^4 r_i\,dr_i]\;[\prod_{i=1}^4 d\alpha_i]}{(\pi r^2)^4} \tag{16}$$

Equations (9)–(12) may be combined to yield

$$C(X) = \overline{\cos(\theta_c)} = 16\int_0^1\int_0^1\int_0^1\int_0^1\int_0^1\int_0^1\int_0^1\int_0^1 \frac{g_1(a_1,a_2,a_3,a_4,s_1,s_2,s_3,s_4)}{g_2(a_1,a_2,a_3,a_4,s_1,s_2,s_3,s_4)}\prod_{i=1}^4 a_i\,da_i\,ds_i \tag{17}$$

where $a_i = r_i/r, s_i = \alpha_i/2\pi$ and

$$g_1(a_1,a_2,a_3,a_4,s_1,s_2,s_3,s_4) = \left[\sum_{i=1}^{2}\sum_{j=3}^{4}(-1)^{i+j}a_ia_j\cos(2\pi(s_i - s_j))\right] - X^{-2} \tag{18}$$

$$g_2(a_1,a_2,a_3,a_4,s_1,s_2,s_3,s_4) = [(a_1^2 + a_2^2 - 2a_1a_2\cos(2\pi(s_2 - s_1)) - X^{-2})\cdot (a_3^2 + a_4^2 - 2a_3a_4\cos(2\pi(s_4 - s_3)) + X^{-2})]^{1/2} \tag{19}$$

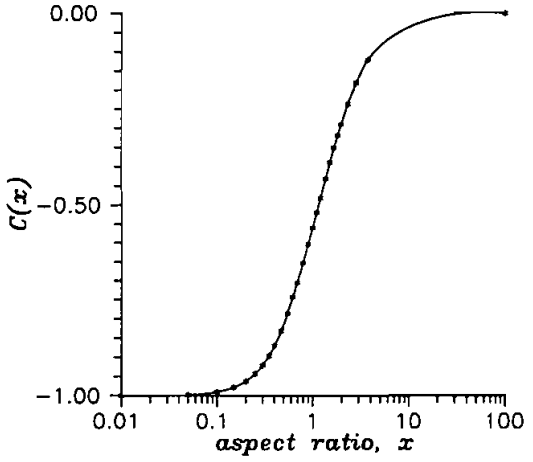

FIGURE 4 Computed and fitted results for $C(X)$. Solid line represents Eq. (17) while symbols the fitted values based on Eq. (48).

Figure 4 depicts the behaviour of $C(X)$, shown as the solid line, obtained from Eqs. (17)–(19) with the integral in each dimension evaluated using finite element quadrature. For small values of X the average value of $\cos(\theta_c)$ is -1 as expected, while for large X the value of $C(X)$ approaches 0. The bulk of the change on increasing the aspect ratio has, however, occurred by $X = 5$, at which point there is negligible correlation among the forward and reverse trajectories. Further it is also evident that there is negligible effect of pore width for $x \leqslant 0.2$, with $C(X) \cong -1$ in this range.

Based on the value of $\overline{\cos(\theta_c)}$ evaluated above (i.e. $C(X)$) it is now possible to estimate the value of $\langle \cos(\theta_c) \rangle$, and hence the correlation factor F, for any network. As mentioned above for the cubic and randomly overlappling capillary networks $F = 1$, due to effect of opposing pore segments. For networks of randomly oriented capillaries with coordination number N, however, $\langle \cos(\theta_c) \rangle = C(X)/N$, since the probability of returning from an intersection into the pore just traversed is $1/N$, and for the remaining randomly oriented pores $\langle \cos(\theta_c) \rangle = 0$. Consequently, following Eq. (5)

$$F = \frac{N + C(X)}{N - C(X)} \tag{20}$$

for N-coordinated networks with randomly oriented pores. Equations (2), (6), (12) and (20) may now be combined to provide the effective diffusivity in such networks in terms of X and ε. Clearly the result is also valid for symmetric networks but with $C(X)$ taken as 0. Before the result is usable, however, it is necessary to relate X and ε. For this it is necessary to construct a suitable mathematical model of the structure, as described in the next section.

Structural Modelling

In the structural models developed here one of the considerations has been the criterion $X \to \infty$ as $\varepsilon \to 1$ so that, as expected, $\langle \cos^2(\theta) \rangle \to 1$ in this limit. This necessitates the inclusion of pore intersections in the modelling.

Cubic Network

A convenient framework for modelling porous medium structure has been provided by Petersen (1957) who assumed that for a network of intersecting cylindrical pores

$$\varepsilon = \pi r^2 L - \frac{k}{3} r^3 \tag{21}$$

where k is a structural constant such that the second term in the right hand side quantifies the loss in volume due to intersections, and L the total length of pore axes per unit volume. The second term in Eq. (21) accounts for loss at intersections. Differentiation of Eq. (21) with respect to r yields the surface area per unit volume given by

$$S = 2\pi r L - k r^2 \tag{22}$$

To evaluate k Petersen used the condition that $S = 0$ at $\varepsilon = 1$, which provides

$$k = \left[\frac{4\pi^3 L^3}{3} \right]^{1/2} \tag{23}$$

following which Eqs. (21) and (22) simplify to

$$\varepsilon = \pi r^2 L \left(1 - \frac{1}{G} \right) \tag{24}$$

$$S = 2\pi r L \left(1 - \frac{3}{2G} \right) \tag{25}$$

where

$$G = \frac{3\pi L}{kr} \tag{26}$$

and satisfies the cubic equation

$$\frac{4}{27} \varepsilon G^3 - G + 1 = 0 \tag{27}$$

Equations (23)–(27) are quite general and, while originally developed (Petersen, 1957) for application to a random network, may be used for other systems if the appropriate value of L is specified.

For a cubic network one has

$$L=\frac{3}{\ell_a^2} \tag{28}$$

where ℓ_a is the length of one edge of a cubic unit cell, so that Eqs. (23) and (26) yield

$$k=\frac{6\pi^{3/2}}{\ell_a^2} \tag{29}$$

$$G=\frac{3}{2y\sqrt{\pi}} \tag{30}$$

where $y=r/\ell_a$. Substitution of Eq. (30) into Eq. (27) now provides

$$2\pi^{3/2}y^3-3\pi y^2+\varepsilon=0 \tag{31}$$

which relates y to ε. Of the three solutions of Eq. (31) one is negative for $\varepsilon>0$, while another lies on a branch for which $y=3/2\sqrt{\pi}$ at $\varepsilon=0$ which is also unacceptable. Consequently, only solutions on the middle branch are meaningful, and these will be discussed in a later section.

It may be noted that the aspect ratio y, based on length of the unit cell, differs from the aspect ratio X required in Eqs. (12) and (20). The latter is based on the effective diffusion length in the pores which is smaller than the length of the unit cell, ℓ_a, because of intersection and overlap effects. It may be expected that the diffusion length in a pore becomes negligibly small as the porosity approaches unity, so that the surface area expression in Eq. (25), which has similar behaviour, may be used to estimate this as

$$\frac{\ell}{\ell_a}=1-\frac{3}{2G} \tag{32}$$

which combines with Eq. (30) to yield

$$X=\frac{y}{(1-y\sqrt{\pi})} \tag{33}$$

Equation (2) may now be used to estimate the dimensionless effective transport coefficient for the cubic network as

$$K_e^*=\varepsilon\gamma^{-1} \tag{34}$$

where γ^{-1} is obtained from Eqs. (3), (12), (31) and (33).

Randomly Oriented Capillaries

In this network the structural elements comprise of randomly oriented capillaries. It is assumed that each node, or intersection, has a coordination number N, and each capillary has a uniform axial length ℓ_a and radius r. In actuality the pores must have a distribution of lengths if they lie between randomly located intersections in the

solid. However the dominant effect is that of the random pore orientations, and for simplicity we therefore assume a constant pore length equal to the expected value of the median at an intersection. It is possible to relate this expected value to the density of pore intersections n by considering the intersections as being randomly located according to a Poisson process. Consequently the probability distribution for the length of the $(N/2+1)$th pore at an intersection is given by

$$P(R)=\frac{\exp\left(-\frac{4\pi R^3 n}{3}\right)\left(\frac{4\pi R^3 n}{3}\right)^{N/2} 4\pi R^2 n}{(N/2)!} \tag{35}$$

which yields the expected value

$$\begin{aligned}\ell_a &= \int_0^\infty RP(R)dR \\ &= \left(\frac{3}{4\pi n}\right)^{1/3}\frac{\Gamma(\frac{N}{2}+\frac{4}{3})}{\Gamma(\frac{N}{2}+1)}\end{aligned} \tag{36}$$

where $\Gamma(X)$ is the gamma function

$$\Gamma(X)=\int_0^\infty t^{(x-1)}e^{-t}dt \tag{37}$$

Equation (36) now provides the total length of pore axes per unit volume as

$$\begin{aligned}L &= \frac{N}{2}\ell_a n \\ &= \frac{s}{\pi\ell_a^2}\end{aligned} \tag{38}$$

where

$$s=\frac{3N}{8}\left[\frac{\Gamma(\frac{N}{2}+\frac{4}{3})}{\Gamma(\frac{N}{2}+1)}\right]^3 \tag{39}$$

As for the case of the cubic lattice we substitute the above value of L into Eqs. (23), (26), (27) and (32) to obtain

$$\frac{2s^{3/2}}{3\sqrt{3}}y^3 - sy^2 + \varepsilon = 0 \tag{40}$$

$$X=\frac{y}{(1-y\sqrt{s/3})} \tag{41}$$

providing the needed relation between the diffusional aspect ratio X and porosity ε. The dimensionless effective transport parameter may now be estimated by means of Eq. (34) with γ^{-1} being obtained from Eqs. (6), (12), (17), (20), (40) and (41).

Randomly Overlapping Capillaries

This kind of structure differs from the previous two in that the capillaries are randomly overlapping and piercing each other in cross-linked fashion. Such a model for the porous solid was first proposed by Bhatia and Perlmutter (1980) and Gavalas (1980), and considers the pore volume as randomly located in the solid, leading to

$$\varepsilon = 1 - \exp(-\pi r^2 L) \tag{42}$$

$$S = 2\pi r L(1-\varepsilon) \tag{43}$$

Gavalas also showed that the mean length between intersections is given by

$$\ell_a = \frac{1}{n_1} \tag{44}$$

where n_1 is the number of intersections per unit length, and is related to the total length of pore axes per unit volume, L, by

$$n_1 = \pi L r \tag{45}$$

Equations (42) and (44), (45) now combine to yield

$$y = -\ln(1-\varepsilon) \tag{46}$$

which in conjunction with Eq. (43), provides

$$X = \frac{-\ln(1-\varepsilon)}{(1-\varepsilon)} \tag{47}$$

As for the cubic network $F = 1$ in the present case as well, and the effective transport coefficient is estimated by means of Eqs. (34), with γ^{-1} following Eqs. (3), (12) and (47).

RESULTS AND DISCUSSION

Structural Modelling

The structural models discussed above relate the diffusional aspect ratio X to the porosity ε. Figure 5 depicts the calculated $X-\varepsilon$ relationship for each of the three cases. For the case of randomly oriented capillaries a coordination number of $N = 6$ was chosen and, as seen in the figure, gave an aspect ratio very close to that of the cubic network. In all cases $X \to \infty$ as $\varepsilon \to 1$ which is the desired effect, as $\langle \cos^2(\theta) \rangle \to 1$ in this limit following Eq. (12). In general, except for very low porosities, the network of randomly overlapping capillaries gave significantly higher aspect ratio compared to the other two structures. This is predominantly due to the lower coordination number of 4 for randomly overlapping capillaries, leading to a smaller number density of pore segments. In confirmation of this, reduction in coordination number N for the network of randomly oriented pore segments also yielded an increase in aspect ratio X, as seen in Figure 6.

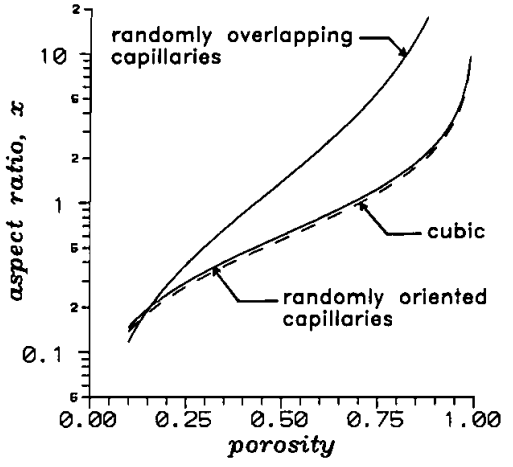

FIGURE 5 Variation of aspect ratio X with porosity for various structural models.

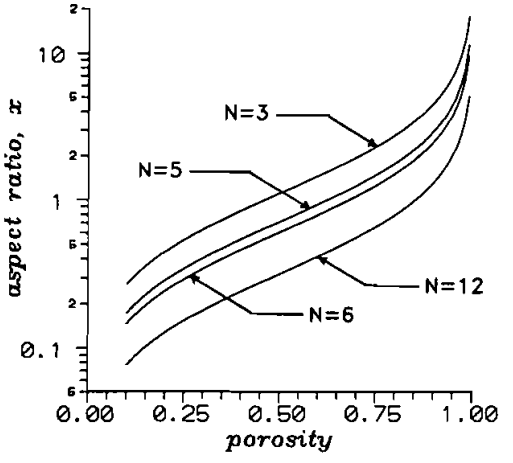

FIGURE 6 Effect of coordination number on variation of aspect ratio X with porosity, for network of randomly oriented intersecting pore segments.

Transport Coefficient

Proposed models

Using the aspect ratio-porosity relationships developed in the earlier section and depicted above, predictions were made for the effective diffusivity for each of the three structures considered here. The results were also compared with the extensive data of Currie (1960) for the effective diffusion coefficient of hydrogen in packed beds of various granular materials. The solid line in Figure 7 depicts the results for a cubic network obtained using Eqs. (3), (12), (31), (33) and (34), while the symbols

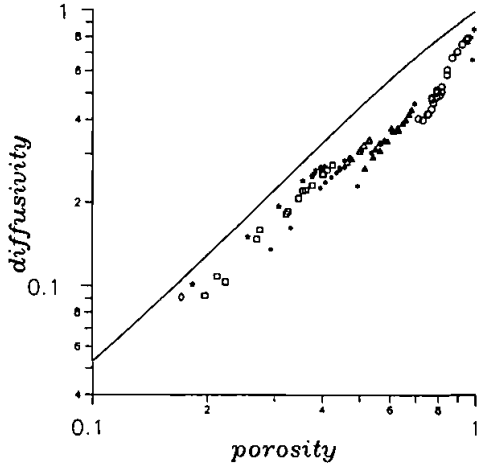

FIGURE 7 Comparison of model predictions, using a cubic network model, for the variation of effective diffusivity with porosity, with experimental data of Currie (1960).

represent the data of Currie. The agreement between the model and data is marginal for the majority of the data, with about 10–30 percent overprediction for much of the data below a porosity of about 0.4. Above a porosity of about 0.5 the deviation is significantly larger with overpredictions as much as 50 percent. Some of Currie's data was taken for packed beds comprised of flaky material such as mica, perspex and vermiculite, or pumice stones of wide size distribution. Such flaky material would have anisotropic diffusivities, due to preferential packing in layers, with the diffusivity in the axial direction being lower than that in the lateral one. Such data was therefore not considered for the model comparisons. The deviation for the other data above about 0.52 porosity (filled triangles, open circles and asterisks) may also be due to shape effects leading to differences in pore geometry, as a small drop in effective diffusivity is evident in the change from one material to another at $\varepsilon \cong 0.52$. In the region below this porosity the materials were regular shaped powders such as sand, sodium chloride, carborundum or glass spheres. Above this porosity the filled circles represent various soil crumbs, while the open circles represent talcs and asterisks highly porous materials such as steel wool and plaster of paris. A small drop in diffusivity is also evident in the switch over from soils to talcs at about $\varepsilon = 0.7$, again pointing to a small contribution from particle shape. This effect is not explicitly represented here, though it may be captured by the choice of a different structural model.

Calculations of the effective diffusivity were also performed here for the network comprising of intersecting randomly oriented pore segments, using Eqs. (6), (12), (17), (20) and (39)–(41). For convenience in the computations the results for $C(X)$ were first curve fitted by a Pade' approximation of the form

$$C(X) = -\frac{1 + 1.08219X + 4.32997 \times 10^{-3} X^2}{[1.04176X + 1.30966X^2 + 0.368099X^3 + 1]} \tag{48}$$

which was subsequently used in the diffusivity calculations. The symbols in Figure 4 represent values predicted by Eq. (48). Figure 8 compares the results for the effective diffusivity predicted by the present model, depicted by the solid line, using a coordination number of $N = 6$, with the experimental data of Currie (1960). This value of N is generally considered appropriate for a variety of porous media, including packed beds, and has been chosen by other workers as well (Burganos and Sotirchos, 1987). It is also consistent with the value for a cubic network. The model predictions appear to match the data upto a porosity of about 50 percent remarkably well and significantly better than the cubic structure presented in Figure 7. Thus, at least for the regular shaped materials used in the lower porosity (below about 50 percent) data the randomly intersecting pore segment model is suitable in describing the pore structure. This is perhaps a result of the random packing of the particles. Figure 9 shows the effect of varying the coordination number of the effective diffusivity predictions. Between $N = 3$ and $N = 6$ the diffusivity increases slightly with increase in N, but for the large value of $N = 12$ the trend is reversed and the diffusivity decreases. This reversal may be explained by the lower aspect ratio for larger N (c.f. Figure 6) which then dominates since the correlation factor F approaches unity as N increases (c.f. Eq. (20)).

Figure 10 shows the results obtained using the randomly overlapping capillary model following Eqs. (3), (12), (34) and (47). This model appears to also predict significantly higher diffusivities over the whole range of conversions in comparison to the experimental data. Clearly this is not an appropriate structure model for packed beds.

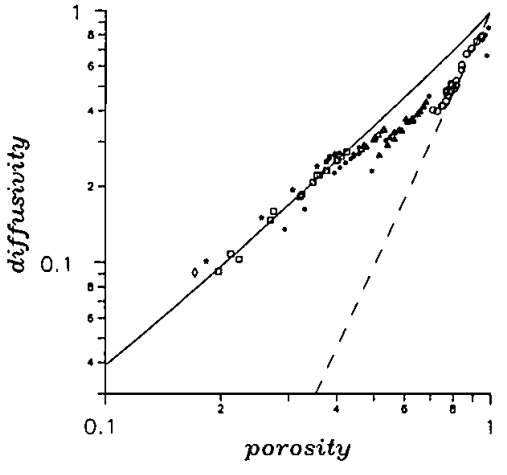

FIGURE 8 Comparison of model predictions, using a model of randomly oriented intersecting pore segments (solid line) and effective medium theory (dashed line), for the variation of effective diffusivity with porosity, with experimental data of Currie (1960).

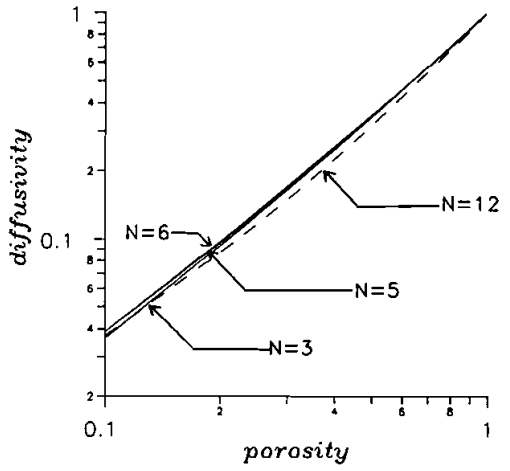

FIGURE 9 Effect of coordination number on variation of effective diffusivity with porosity, for a network of randomly oriented pore segments.

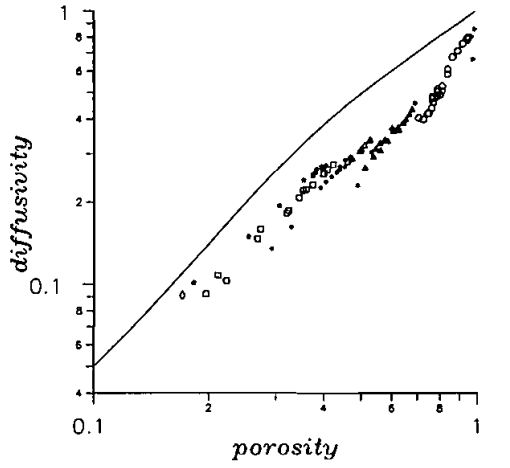

FIGURE 10 Comparison of model predictions, using a model of randomly overlapping capillaries, for the variation of effective diffusivity with porosity, with experimental data of Currie (1960).

Comparison with Prior Models

For purposes of comparison calculations were also done for the variation of the effective diffusion coefficient using several prior models of transport in unconsolidated media. The dashed line in Figure 8 represents the results from effective medium theory (Bruggeman, 1935; Landauer, 1952) for a mixture of several phases,

$$\sum_i \phi_i \left(\frac{K_i - K_e}{K_i + 2K_e} \right) = 0 \tag{49}$$

which for our case yields

$$\frac{K_e}{K} = \frac{3\varepsilon - 1}{2} \tag{50}$$

Clearly the effective medium theory performs very poorly, and appears to be in agreement with the data only above about $\varepsilon = 0.7$. In the same range the six-coordinated network of randomly intersecting capillaries does not perform equally well, while being much closer to the data below $\varepsilon = 0.7$.

Figure 11 compares the data of Currie and predictions from the well-known result of Rayleigh (1892)

$$\frac{K_e}{K} = \frac{[2\varepsilon - 0.3938\,(1-\varepsilon)^{10/3}]}{[(3 - \varepsilon - 0.3938\,(1-\varepsilon)^{10/3}]} \tag{51}$$

given as the dashed curve, as well as of its modification by Meredith and Tobias (1961)

$$\frac{K_e}{K} = \frac{[2\varepsilon + 1.227\,(1-\varepsilon)^{7/3} - 1.6\,(1-\varepsilon)^{10/3}]}{[(3 - \varepsilon + 1.227\,(1-\varepsilon)^{7/3} - 1.6\,(1-\varepsilon)^{10/3}]} \tag{52}$$

given as the solid curve. In both cases the predictions are relatively poor compared to those of the randomly intersecting pore network model developed here. Somewhat better agreement is seen for Weissberg's model (1963)

$$\frac{K_e}{K} = \varepsilon/[1 - 0.51n\,(\varepsilon)] \tag{53}$$

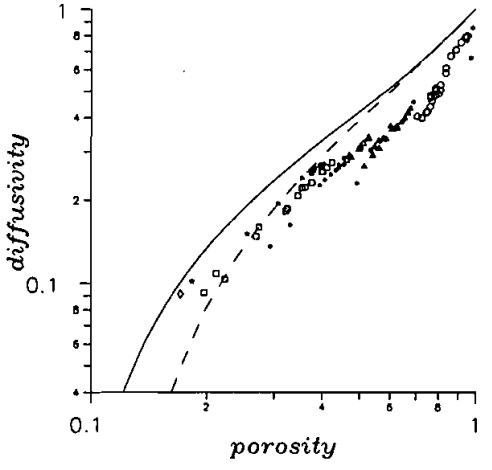

FIGURE 11 Comparison of predictions from Meredith and Tobias' (1961) model (solid line) and Rayleigh's (1892) model (dashed line), for the variation of effective diffusivity with porosity, with experimental data of Currie (1960).

depicted by the solid line in Figure 12. However, in the same range ($\varepsilon < 0.4$) where this model performs the best the randomly intersecting pore network model does considerably better, while also having somewhat better agreement above a porosity of 0.4 (c.f. Fig. 8). Also shown in Figure 12 as the dashed curve is the result from Prager's (1963) expression

$$\frac{K_e}{K} = \frac{\varepsilon(1+\varepsilon)}{2} \tag{54}$$

which is somewhat poorer than Weissberg's result.

Figure 13 depicts the results from Bruggeman's (1935) recommendation

$$\frac{K_e}{K} = \varepsilon^{3/2} \tag{55}$$

as the solid line, and from Maxwell's (1892) early expression

$$\frac{K_e}{K} = \frac{2\varepsilon}{(3-\varepsilon)} \tag{56}$$

given as the dashed line. The latter has in more recent times been theoretically supported by Neal and Nader (1973) but performs poorly against the data of Currie. In comparison the Bruggeman result is superior, almost matching the performance of our randomly intersecting pore network. The latter, however, does yield better agreement over the entire porosity range.

It is clear from the above results that the intersecting pore network model developed here is superior to the earlier expressions. Further development of this model to include the Knudsen effect and pore size dependent diffusivities, along with

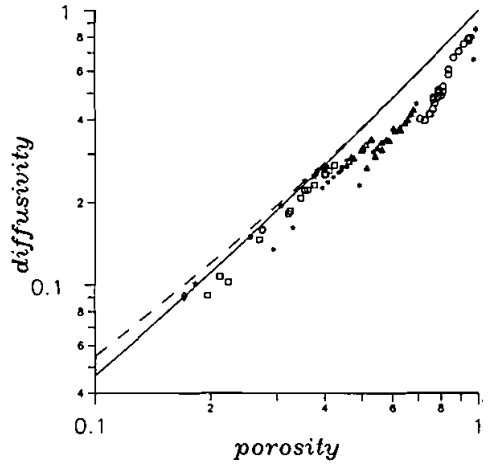

FIGURE 12 Comparison of predictions from Weissenberg's (1963) model (solid line) and Prager's (1963) model (dashed line), for the variation of effective diffusivity with porosity, with experimental data of Currie (1960).

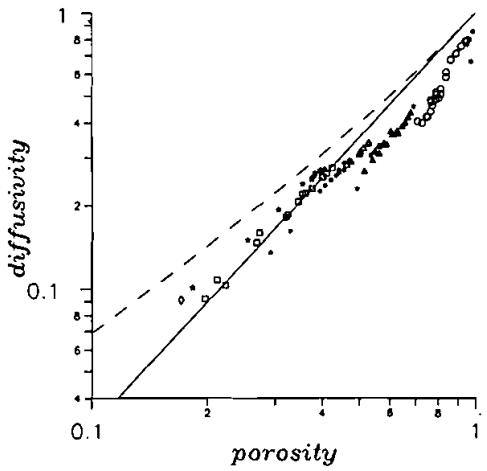

FIGURE 13 Comparison of predictions from Bruggemann's (1935) model (solid line) and Maxwell's (1892) model dashed line), for the variation of effective diffusivity with porosity, with experimental data of Currie (1960).

consideration of the aspect ratio, is therefore an attractive prospect for future work. This will then permit improved predictions also for consolidated porous media such as catalyst pellets, coal chars and adsorbents which are strongly microporous.

SUMMARY AND CONCLUSIONS

The conventional model for the estimation of the tortuosity factor for transport in porous media is modified here to account for a non-zero aspect ratio of the pores. Three different structural models have been used to estimate the aspect ratio as a function of porosity. It is seen that the aspect ratio has a strong influence on the tortuosity factor which reduces with increase in porosity, as expected. Comparison of predicted effective diffusivities with experimental data for diffusion in packed beds showed that a suitable structural model in terms of capillary networks, such as that of a network of randomly oriented intersecting pore segments, may be used to interpret the data. The predictions of this model match the data of Currie (1960) for diffusion in packed beds better than previously existing ones for unconsolidated media. Extension of the network approach to incorporate pore size dependent diffusivities with the aspect ratio is therefore desirable.

ACKNOWLEDGEMENT

This research was conducted while the author held a visiting appointment at the Department of Chemical Engineering, Technical University of Denmark, during 1994. Support of this position by the Danish Research Council is gratefully acknowledged.

NOTATION

(Symbols that do not appear here are defined in the text)

$\mathbf{F}$	correlation factor
G	constant, Eq. (26)
$\mathbf{i}, \mathbf{j}, \mathbf{k}$	unit cartesian vectors
J	flux
k	structural constant
$\bar{K}$	mean transport coefficient in pores
K_e	effective transport coefficient
ℓ	diffusion length in pore
ℓ_a	actual length of the axis
L	total length of pore axes per unit volume
n	number of pore intersections per unit volume
n_1	number of intersections per unit pore length
N	coordination number
$p(\theta)$	probability distribution for θ
q	field variable
r	pore radius
S	surface area per unit volume
X	effective or diffusional aspect ratio, r/ℓ
y	r/ℓ_a
z	axial coordinate

Greek Letters

α	azimuthal angle
ε	porosity
γ	tortuosity factor
ϕ_i	volume fraction of the ith phase
θ	angle between net diffusion direction in the pore and macroscopic flux vector
θ_1	$\tan^{-1}(2r/\ell)$
θ_2	angle between pore axis and macroscopic diffusion direction
θ_c	angle between successive steps

REFERENCES

Akanni, K. A., Evans, J. W. and Abramson, I. S., "Effective Transport Coefficients in Heterogeneous Media," *Chem. Engng. Sci.*, **42**, 1945 (1987).

Bhatia, S. K., "Directional Autocorrelation and the Diffusional Tortuosity of Capillary Porous Media," *J. Catalysis*, **93**, 192 (1985).

Bhatia, S. K., "Stochastic Theory of Transport in Inhomogeneous Media," *Chem. Engng. Sci.*, **41**, 1311 (1986).

Bhatia, S. K. and Perlmutter, D. D., "A Random Pore Model for Fluid-Solid Reactions: I. Isothermal Kinetic Control," *A. I. Ch. E. J.*, **26**, 379 (1980).

Bruggemann, D. A. G., "Berechnung Vrschiedener Physicalischer Konstaten von Heterogenen Substanzen," *Ann. Physik*, **24**, 636 (1935).

Burganos, V. N. and Sotirchos, S. V., "Diffusion in Pore Networks: Effective Medium Theory and Smooth Field Approximation," *A. I. Ch. E. J.*, **33**, 1678 (1987).
Currie, J. A., "Gaseous Diffusion in Porous Media: Part 2.-Dry Granular Materials," *British J. Appl. Phys.*, **11**, 318 (1960).
Deepak, P. D. and Bhatia, S. K., "Transport in Capillary Network Models of Porous Media: Theory and Simulation," *Chem. Engng. Sci.*, **49**, 245 (1994).
Gavalas, G. R., "A Random Capillary Model with Application to Char Gasification at Chemically Controlled Rates," *A. I. Ch. E. J.*, **26**, 577 (1980).
Jackson, R., *Transport in Porous Catalysts*, Elsevier, Amsterdam (1977).
Johnson, M. F. L. and Stewart, W. E., "Pore Structure and Gaseous Diffusion in solid Catalysts," *J. Catalysis*, **4**, 248 (1965).
Landauer, R., "The Electrical Resistance of Binary Metallic Mixtures," *J. Appl. Phys.*, **23**, 779 (1952).
Le Claire, A. D., "Diffusion," in *Treastise on solid state chemistry*, **4**, Reactivity of Solids, Hannay, N. B. ed., New York, p1 (1976).
Mason, E. A. and Malinauskas, A. P., *Gas Transport in Porous Media: The Dusty Gas Model*, Elsevier, Amsterdam (1983).
Maxwell, J. C., *Electricity and Magnetism*, Clarendon Press, Oxford (1892).
Meredith, R. E. and Tobias, C. W., "Conductivities in Emulsions," *J. Electrochem. Soc.*, **108**, 286 (1961).
Neal, G. H. and Nader, W. K., "Prediction of Transport Processes within Porous Media: Diffusive Flow within a Homogeneous Swarm of Spherical Particles," *A. I. Ch. E. J.*, **19**, 112 (1973).
Petersen, E. E., "Reaction of Porous Solids," *A. I. Ch. E. J.*, **3**, 445 (1957).
Pismen, L. M., "Diffusion in Porous Media of a Random Structure," *Chem. Engng. Sci.*, **29**, 1227 (1974).
Prager, S., "Diffusion and Viscous Flow in Concentrated Suspensions," *Physica*, **29**, 129 (1963).
Rayleigh, Lord, "On the Influence of Obstacles Arranged in Rectangular Order Upon the Properties of a Medium," *Phil. Mag.*, **34**, 481 (1892).
Sahimi, M., Gavalas, G. R. and Tsotsis, T. T., "Statistical and Continuum Models of Fluid-Solid Reaction in Porous Media," *Chem. Engng. Sci.*, **45**, 1443 (1990).
Tomadakis, M. M. and Sotirchos, S. V., "Ordinary, Transition and Knudsen Regime Diffusion in Random Capillary Structures," *Chem. Engng. Sci.*, **48**, 3323 (1993).
Weissberg, H. L., "Effective Diffusion Coefficient in Porous Media," *J. Appl. Phys.*, **34**, 2636 (1963).